POLITECNICO
MILANO 1863

SCUOLA DI INGEGNERIA INDUSTRIALE
E DELL'INFORMAZIONE

Izmit Bay Bridge aeroelastic analysis

Wind Engineering project

Group A

Nicola Caldieraro, 245826
Marco Corbelli, 245320
Giovanni Orazi, 247368
Elisa Piergiacomi, 259148
Luca Piomboni, 242588

Academic year:
2023-2024

Date of delivery:
July 2024

Abstract: Wind-structure interaction is one of the main aspects in Bridges' design and test phases. This study aims to analyze the behaviour of the Izmit Bay Bridge under the action of static and dynamic stresses due to the local wind flow with a particular focus on the dynamic instabilities of the system under the action of an external Buffeting exciting term. Analysis on both sectional and full bridge models have been performed

1. Introduction

1.1. Wind Bridge interaction

The analysis of the behaviour of bridges subjected to aerodynamic loads, both static and dynamic, is critical during the design phase of the structures. These types of interaction are highly nonlinear due to the intrinsic nonlinearity of turbulence and its interaction with the structure's dynamic reaction. Therefore, the development of numerical models capable of predicting the rise of aeroelastic phenomena, such as static divergence, flutter, and buffeting is essential. Our work aims to provide an overview of the different models that can be employed to predict such phenomena, evaluating their capability. Wind-induced forces on bridge decks are represented as the sum of buffeting (aerodynamic) force, related to the approaching wind-velocity fluctuations, and the self-excited (aeroelastic) force, generated by the bridge deck motions. In the first part of the analysis, a steady model is used to describe the static loads on the bridge. On the other hand, to effectively describe the dynamics of the system it is necessary to include the nonlinear nature of the aeroelastic problem. Hence, a quasi-steady model is applied in the aeroelastic analysis of bridges. Within this approach, the aeroelastic forces are nonlinear functions of the effective angle of attack, meaning the combination of the bridge deck motions and approaching wind-velocity fluctuations.

1.2. Quasi-steady approach

The quasi-steady approach simplifies the complex interaction between aerodynamic forces and the structural response by assuming that the aerodynamic forces at any given instant are similar to the forces that would be

present under steady-state conditions at that same instant. This assumption is particularly useful when the wind speed or bridge displacement changes slowly compared to the time it takes for the aerodynamic forces to adjust to these changes.
The key assumptions are:

- Slow Variation of Forces: It is assumed that the aerodynamic forces change slowly with time, allowing for a near-instantaneous adjustment to the current state of the structure.
- Steady-State Forces: Aerodynamic forces are calculated as if the flow around the structure is steady, even though it may be changing slowly with time.
- Simplified Analysis: By assuming steady-state conditions, the analysis becomes less complex and more tractable, avoiding the need for fully dynamic aerodynamic simulations.

The limitation of this approach is in terms of accuracy in the prediction of forces under rapidly changing conditions or highly turbulent wind flows, and the fact that it may oversimplify complex aeroelastic interactions, leading to less precise results for dynamic stability analysis.

1.3. Von Karman Spectrum

The main character of the treated analysis is the interaction between wind and structures. To perform reliable computations of the parameters of interest there is the need to consider the real nature of the external forcing term, the wind. It's not a deterministic quantity since we cannot use a mathematical law with predetermined parameters to describe its behaviour. Hence we need to analyze this stochastic phenomenon using statistical tools applied to data recovered through measurement sessions performed in the area of interest. To perform such analysis we need the following data.

1.3.1. Wind speed profile

The behaviour of the structure depends on the external exciting terms. These are functions of the wind speed that's acting on the bridge. Performing a measurement of the wind speed at different heights an approximated representation of the local wind profile is obtained. There is the opportunity to relate the wind speed intensity at a specific height to a reference value used in our computation. The height of interest is the one of the bridge's desk and is changing along the span of the bridge itself.

1.3.2. Turbulence intensity

In the atmospheric boundary layer, the wind is always turbulent, hence the flow is irregular and chaotic. Consequently, statistical methods are needed to describe its average behaviour. Knowing the mean wind speed value and monitoring the speed values in time the *Level of turbulence* is obtained through horizontal standard deviation computation.

$$\sigma_u = \left\{ \frac{1}{T} \int_0^T [U(t) - U]^2 dt \right\}^{\frac{1}{2}} \tag{1}$$

The standard deviations for the lateral and vertical turbulence components are related to the vertical one as follows

$$\sigma_v \approx 0.75\sigma_u \tag{2}$$

$$\sigma_w \approx 0.5\sigma_u \tag{3}$$

The *Turbulence Intensity* is defined as the ratio between the standard deviation previously computed and the mean velocity, hence it's a non-dimensional number. Both are functions of the height z so we have the following
Longitudinal Turbulence Intensity

$$I_u(z) = \frac{\sigma_u(z)}{U(z)} \tag{4}$$

Lateral Turbulence Intensity

$$I_v(z) = \frac{\sigma_v(z)}{U(z)} \tag{5}$$

Vertical Turbulence Intensity

$$I_w(z) = \frac{\sigma_w(z)}{U(z)} \tag{6}$$

1.3.3. Integral length scale

The last parameter needed to describe the turbulent behaviour of the wind is the average size of the gust in a given direction that could be interpreted as the measure of the size of the vortices in the wind and is computed along the three orthogonal directions for each speed component
The analysis performed neglected the presence of the wind speed component in the bridge's span direction so both *turbulence intensity* and *integral length scale* are considered about the u and w wind speed components only.

1.3.4. Power spectral density

The stochastic process that defines the air motion is characterized by a certain energy content that could be computed in the frequency domain through the *Power Spectral Density (PSD)* $\Phi_{XX}(\omega)$ which is defined as the Fourier transform of the *Autocorrelation* $k_{XX}(\tau)$ of the process itself. This last quantity defines the link, for an ergodic process, between a signal and itself shifted in time of a certain time interval τ. If τ the Autocorrelation coincides with the variance of the signal analyzed. In other words, the PSD describes the frequency content of a random process and it's computed as follows

$$\Phi_{XX}(\omega) = F[k_{XX}(\tau)] = \int_{-\infty}^{+\infty} k_{XX}(\tau) e^{-j\omega\tau} d\tau \tag{7}$$

Since $k_{XX}(\tau) \propto X^2$ the PSD is an expression of the energy content of the signal X.
The frequency distribution of turbulence along the wind velocity component is described through the non-dimensional PSD function $\frac{f \cdot S_u(f)}{\sigma_u^2}$. The most commonly used for wind component is the *Von Karman Spectrum* defined as follows for $u(t)$

$$\frac{f \cdot S_u(f)}{\sigma_u^2} = \frac{4(\frac{f^x L_u}{U})}{[1 + 70.8(\frac{f^x L_u}{U})^2]^{\frac{5}{6}}} \tag{8}$$

The Von Karman PSD for $w(t)$ is the following one

$$\frac{f \cdot S_w(f)}{\sigma_w^2} = \frac{4(\frac{f^x L_w}{U})(1 + 755.2(\frac{f^x L_w}{U})^2)}{[1 + 283.2(\frac{f^x L_w}{U})^2]^{\frac{11}{6}}} \tag{9}$$

1.4. Flutter

Flutter is a typical aeroelastic phenomenon that occurs in flexible structures like wings, bridges, helicopter blades, etc. This instability may occur when the system one is analysing is characterised by more than one degree of freedom. It is the result of the coupling of inertia, aerodynamics and aeroelasticity. Moreover, one needs bending and torsion to be coupled to experience flutter.
We shall undergo a more detailed description of the instability.

1.4.1. Eigen analysis

The equation that describes the motion of a generic body in a fluid dynamic field is the following:

$$\boldsymbol{M}\ddot{q}(t) + \boldsymbol{C}\dot{q}(t) + \boldsymbol{K}q(t) = 0 \tag{10}$$

In order to study the phenomenon, one may do the strong assumption to neglect damping and study a simplified equation of motion. This formulation will be handlier to be deployed for the eigenanalysis:

$$\boldsymbol{M}\ddot{q}(t) + \boldsymbol{K}q(t) = 0 \tag{11}$$

One can now set the eigen problem to compute the eigenvalues of the system. We remark that stability problems are keen to be studied through the analysis of the behaviour of the eigenvalues and, more specifically, the behaviour of the real part of it.
Performing the following substitution to move to the frequency domain:

$$q(t) = \hat{q}e^{i\omega t} \tag{12}$$

The equation becomes:

$$(-\omega^2 \boldsymbol{M} + \boldsymbol{K})\hat{q} = 0 \tag{13}$$

Undergoing algebraic manipulation:

$$\det(-\omega^2 \boldsymbol{M} + \boldsymbol{K}) = 0 \tag{14}$$

Now that the generic equation is built, one may add the aerodynamic contribution to stiffness (intermediate passages have been skipped, since the procedure really does depend on the structure taken into account but the purpose of this section is to stick to the most generic case):

$$\boldsymbol{M}\ddot{q}(t) + (\boldsymbol{K} - q\boldsymbol{K}_A)q(t) = 0 \tag{15}$$

where q stands for the dynamic pressure.
This formulation permits to study the behaviour of the sign of the eigenvalues, that will have the following shape:

$$\lambda = \sigma \pm i\omega \tag{16}$$

$$\sigma = \Re(\lambda) \tag{17}$$

And further values may be described: Damping ratio:

$$\xi = -\frac{\Re(\lambda)}{|\lambda|} \tag{18}$$

Natural frequency:

$$\omega_n = \frac{\Im(\lambda)}{\sqrt{1-\xi^2}} \tag{19}$$

The analysis of the stability of the system consists in the study of the sign of the real part of the eigenvalue or, consequently in the study of the sign of the damping ratio.

- Asymptotically stable system: $\xi < 0$
- Stable system: $\xi \leq 0$
- Unstable system: $\xi > 0$

In general, when the real part falls into the positive part of the plane, instability will occur. On the other hand, the oscillating behaviour of the system depends on the imaginary part of the eigenvalue: if it is different from zero, the instability will oscillate. How does it oscillate? One may take a look at the natural frequency.
We end up saying that the flutter is the pressure at which the instability is experienced.

1.4.2. Flutter in Bridges

The typical shape of bridges, as structures endowed with a significantly one longer dimension than the other two, permits this instability to occur.

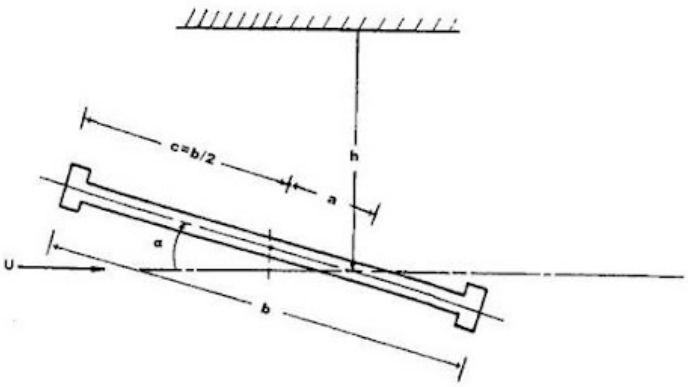

Figure 1: Sectional flutter

Bridges may suffer from two kinds of flutter, classic flutter and stall flutter. In the first case, flutter is a two degrees of freedom instability, while in the second case, flutter is only a torsional instability and is generated by an incident wind flow with a non-null angle of attack.

1.5. Buffeting

Buffeting refers to the dynamic response of a bridge structure to the fluctuations of the wind due to turbulence. It is a type of aeroelastic phenomenon that can cause vibration and oscillations on the bridge that can be controlled by increasing aerodynamic damping or the bridge's stability. This phenomenon is unavoidable in all bridges and structures
The aerodynamic forces due to turbulence can be identified both through wind tunnel tests and through the Quasi Steady Theory. The equation of motion can be written as :

$$[M_{diag}]\ddot{x} + ([R_{diag}] + [R_{aero}])\dot{x} + ([K_{diag}] + [K_{aero}])x = F_{buff} \tag{20}$$

where x represents the displacement of the nodes of the structure and M, R, K are, respectively, the mass, damping and stiffness matrices of the bridge structure.

$$F_{buff} = \frac{1}{2}\rho U^2 B \begin{bmatrix} 2C_{D0} & (K_{D0} - C_{L0}) \\ 2C_{L0} & (K_{L0} + C_{D0}) \\ 2C_{M0}B & K_{M0}B \end{bmatrix} \begin{bmatrix} \frac{u}{U} \\ \frac{w}{U} \end{bmatrix} \tag{21}$$

where B represents the reference body dimension, C_{D0}, C_{L0}, C_{M0} are, respectively, the drag, lift and moment coefficients, K_{D0}, K_{L0}, K_{M0} are their derivatives with respect to the angle of attack, ρ is the air density, U is the velocity vector and u and w are the velocity components.

The aerodynamic equivalent matrices $[K_{aero}]$ and $[R_{aero}]$ and buffeting forces F_{buff} are, at first, derived in the time domain, but, due to wind turbulence's stochastic nature, frequency domain analysis is preferred. Time domain solutions need infinite wind histories for accuracy, but computational limits restrict histories to finite lengths, missing low-frequency variations. In the frequency domain, the buffeting forces must be expressed either in PSD (Power Spectral Density) or FFT (Fast Fourier Transform).

1.6. Izmit Bay Bridge

The Izmit Bay Bridge is a cable-suspended and cable-stayed bridge in Turkey. The design of the aeroelastic model for this bridge requires accurately reproducing aerodynamic and structural properties. Due to the bridge's length of 2682 meters and the wind tunnel's turntable diameter of 13 meters, a length scale of 1:220 was chosen, resulting in a model length of 12191 mm. The scale factors for other physical quantities were calculated based on this length scale. Finite Element Methods (FEM) are used to simulate the prototype and identify the main vibration modes. The model's design focuses on the deck, towers, and cables. After construction, modal identification ensures accurate reproduction of vibration modes.
The deck of bridge model is designed to replicate the wind forces experienced by it. The internal structure uses aluminum for its ease of machining, replicating bending stiffness and torsional stiffness. Due to scale factors and Froude similarity, the model's Reynolds number is significantly lower than the full scale, potentially affecting aerodynamic behavior. Therefore, sectional force coefficients should be measured on both the scaled model and a larger sectional model for comparison.
Bridge's aerodynamic coefficients computed through wind tunnel tests are reported in figure 2

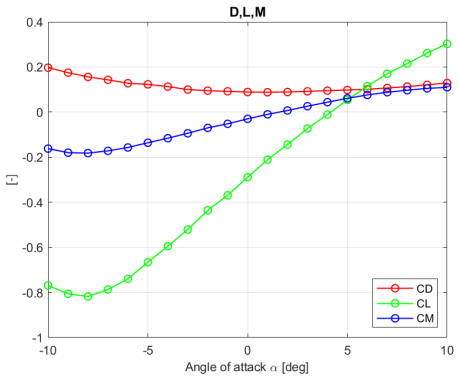

(a) *Static aerodynamic coefficients*

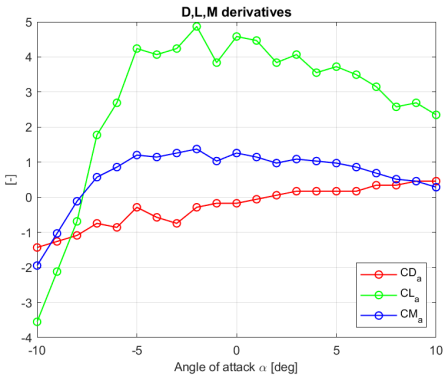

(b) *Static aerodynamic coefficients derivatives*

Figure 2

2. Computations

The data provided regarding the section were:

$$\rho = 1.225 \text{ kg/m}^3, \quad L = 1 \text{ m}, \quad m_z = m_y = m = 23160 \text{ kg/m}, \quad J = 2.77 \times 10^6 \text{ kg m}^2/\text{m},$$
$$f_y = 0.05 \text{ Hz}, \quad f_z = 0.0884 \text{ Hz}, \quad f_t = 0.259 \text{ Hz}, \quad \zeta = 0.004$$

from these data it is possible to compute the following natural frequencies for each independent motion[1]:

$$\omega_y = 2\pi f_y, \quad \omega_z = 2\pi f_z, \quad \omega_t = 2\pi f_t,$$

damping coefficients:

$$r_y = 2m\omega_y\zeta, \quad r_z = 2m\omega_z\zeta, \quad r_t = 2J\omega_t\zeta,$$

and stiffnesses:

$$k_y = \omega_y^2 m_y, \quad k_z = \omega_z^2 m_z, \quad k_t = \omega_t^2 J,$$

the structural matrices were built as follows:

$$\mathbf{M_{str}} = \begin{bmatrix} m & 0 & 0 \\ 0 & m & 0 \\ 0 & 0 & J \end{bmatrix} \quad \mathbf{R_{str}} = \begin{bmatrix} r_y & 0 & 0 \\ 0 & r_z & 0 \\ 0 & 0 & r_t \end{bmatrix} \quad \mathbf{K_{str}} = \begin{bmatrix} k_y & 0 & 0 \\ 0 & k_z & 0 \\ 0 & 0 & k_t \end{bmatrix}$$

where $\mathbf{M}$ is the mass matrix, $\mathbf{R}$ is the damping matrix, and $\mathbf{K}$ is the elastic matrix. Subsequently, the static displacements were computed by solving the linear static equilibrium equations as:

$$\theta_{\text{static}} = \frac{\frac{1}{2}\rho U^2 B^2 C_{M0}}{k_t - \frac{1}{2}\rho U^2 B^2 \cdot C_{m\alpha 0}}, \quad y_{\text{static}} = \frac{\frac{1}{2}\rho U^2 B \cdot C_{d\theta}}{k_y}, \quad z_{\text{static}} = \frac{\frac{1}{2}\rho U^2 B \cdot C_{l\theta}}{k_z}, \tag{22}$$

where B is the section chord. The torsional displacement was also computed with a non-linear approach by employing the script '*statica.m*' provided. This value is later used in the flutter and buffeting computation.
A quasi-steady approach was chosen for the computation of flutter. The contribution to the system's matrix due to the aerodynamic loads was computed as:

$$\mathbf{M_{aero}} = \mathbf{0}, \quad \mathbf{R_{aero}} = \frac{1}{2}\rho U B \begin{bmatrix} 2C_d & (C_{d\alpha} - C_l) & (C_{d\alpha} - C_l)B_1^y \\ 2C_l & (C_{l\alpha} + C_d) & (C_{l\alpha} + C_d)B_1^z \\ B \cdot 2C_m & BC_{m\alpha} & BC_{m\alpha}B_1^t \end{bmatrix}, \quad \mathbf{K_{aero}} = \frac{1}{2}\rho U^2 B \begin{bmatrix} 0 & 0 & -C_{d\alpha} \\ 0 & 0 & -C_{l\alpha} \\ 0 & 0 & -BC_{m\alpha} \end{bmatrix}$$

where the quasi-steady coefficients:

$$B_1^t = 0.3B, \quad B_1^y = 0, \quad B_1^z = 0 \tag{23}$$

and the aerodynamic coefficients were obtained through interpolation of the provided aerodynamic data regarding the section. Hence, the total matrices of the system subjected to aerodynamic loads are:

[1]The bridge's deck has three independent degrees of freedom, i.e. lateral y, vertical z and torsional t motions

$$\mathbf{M} = \mathbf{M_{str}} + \mathbf{M_{aero}}, \quad \mathbf{R} = \mathbf{R_{str}} + \mathbf{R_{aero}}, \quad \mathbf{K} = \mathbf{K_{str}} + \mathbf{K_{aero}},$$

As mentioned in the previous sections, the flutter is studied by solving the eigenproblem associated to the system:

$$\boldsymbol{M}\ddot{q}(t) + \boldsymbol{C}\dot{q}(t) + \boldsymbol{K}q(t) = 0 \tag{24}$$

thus the eigenvalues and eigenvectors were computed using Matlab '*polieig*' function at different velocities. By plotting the damping ratio given by:

$$\xi = -\frac{\mathrm{Re}(\lambda)}{||\lambda||} \tag{25}$$

as a function of the velocities, the flutter velocity was identified as the velocity for which the damping ratio went from positive to negative. For what concerns the buffeting analysis, we consider the same system that was used for the flutter analysis but subjected to a buffeting force given by:

$$\mathbf{F}_{buff} = \frac{1}{2}\rho U^2 B \begin{bmatrix} 2C_{D0} & (K_{D0} - C_{L0}) \\ 2C_{L0} & (K_{L0} + C_{D0}) \\ 2C_{M0}B & K_{M0}B \end{bmatrix} \begin{bmatrix} \frac{u}{U} \\ \frac{w}{U} \end{bmatrix} \tag{26}$$

where u and w are respectively the turbulent fluctuation of the wind in the x and z direction. Since the wind spectrum is known, the computations were carried on in the frequency domain by using the Fourier transform, obtaining:

$$\left[-\omega^2\mathbf{M}(\omega) + i\omega\mathbf{C}(\omega) + \mathbf{K}\right]\mathbf{q}(\omega) = \mathbf{F}_{\mathrm{buff}}(\omega) \tag{27}$$

the expression of the displacements in the frequency domain is:

$$\mathbf{q}(\omega) = \mathbf{H}(\omega)\mathbf{F}_{\mathrm{buff}}(\omega) \tag{28}$$

where $\mathbf{H}(\omega)$ is the transfer function of the system. The solution was computed by fixing the wind mean velocity and solving the equation in a limited bandwidth of frequencies. From the solution, the PSD was computed as:

$$\phi_q(\omega) = |\mathbf{q}(\omega)| \tag{29}$$

and the RMS at different velocities as:

$$g_{\mathrm{RMS}} = \sqrt{\int_{\omega_0}^{\omega_1} \phi_q(\omega)\ d\omega} \tag{30}$$

2.1. Full bridge

The full bridge analysis investigates the 3D solution of what we have already done in the sectional problem. Our purpose is to study the dynamic solution of 4 out of the 14 modes that characterize the full bridge. What is interesting to see is that the results are not totally coincident: for instance, the flutter velocity will be slightly higher in the full bridge. This is due to the mutual interaction of each section that compose the bridge.

3. Conclusions

Analyzing the results obtained from the previously described computations the following observations are obtained.

3.1. Static displacement of the sectional model

As first analysis, the static displacements of the bridge's deck have been computed starting from the aerodynamic coefficients and the stiffness of the deck section. The static configuration is an equilibrium condition, hence imposing the torsional equilibrium, that is function of aerodynamic coefficients, dynamic pressure and structural stiffness, the associated twist angle θ has been computed. This angle could be interpreted as the angle of attack of the deck with respect to the wind flow. Thus vertical and lateral displacements are directly computed through the equations 22. The obtained results are reported in figure 3 that also shows the difference between

the computed θ and the linear one; this difference increases with the mean wind speed highlighting that there is a good approximation for a wide range of stream velocities.

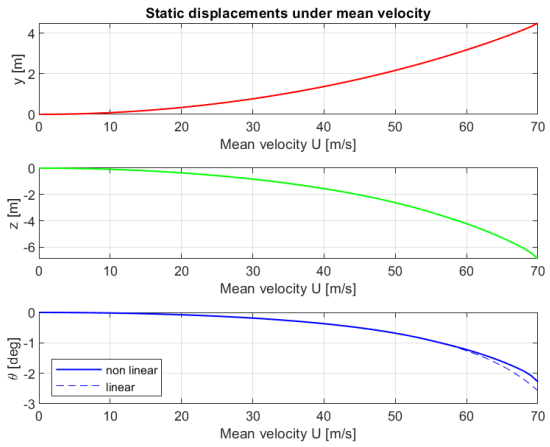

Figure 3: Static displacements of the bridge's cross section

3.2. Sectional model's dynamic response

The aim of this study is to analyze the dynamic instabilities of the Izmit Bay Bridge. The structure is excited by an external forcing term due to wind with a certain turbulence intensity which implies the presence of a buffeting input acting on the deck of the Bridge. The presence of system's instability conditions has been verified through the eigenvalue computation shown in the figure4. Stable behaviours are characterized by a negative, or at least null, eigenvalues' real part ($\Re(\lambda)$) which corresponds to a positive damping ratio condition. Hence the instability is present when the real part of at least one turns positive implying a negative damping condition.

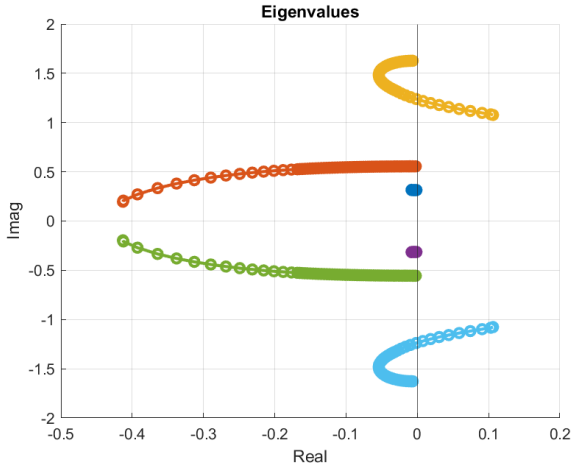

Figure 4: Eigenvalues of the sectional model's dynamic problem

Using the aerodynamic coefficients and the main wind statistical characteristics, the behaviour of the bridge has been analyzed and the system's response highlighted the presence of a flutter condition at a mean wind speed of 61 $\frac{m}{s}$. Indeed, the structural damping of the system for one of the three degrees of freedom crosses the x-axis and starts to become negative for a specific speed value, which by definition is called *Flutter speed*, turning the system from a stable to an unstable dynamic behaviour. This condition is better shown in the figure5 where each degree of freedom's damping is plotted in function of the wind mean speed. The numerical analysis has been performed for a speed range that ends not far from the first identified flutter condition since the main information is the lowest flutter speed. If we extended the computation to a wider speed range we would have identified speeds at which the damping of the other degrees of freedom turns negative, i.e. the successive flutter conditions.

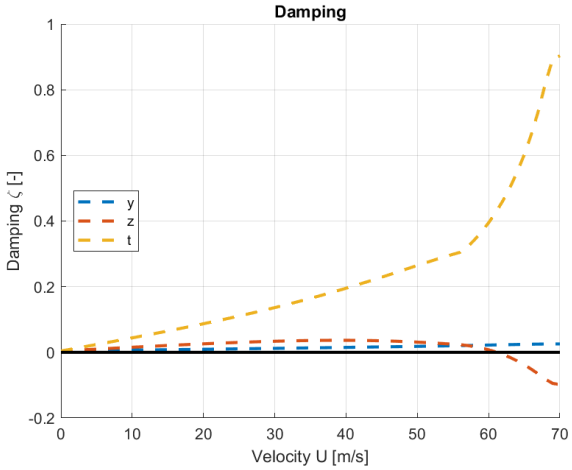

Figure 5: Sectional model Damping

To better identify the flutter condition, analysis in the frequency domain has been performed obtaining, using the computation passages previously described, the system response in frequency domain (i.e. Fourier transform of the response of the system in time domain) which is reported in the following plots in figure 6.

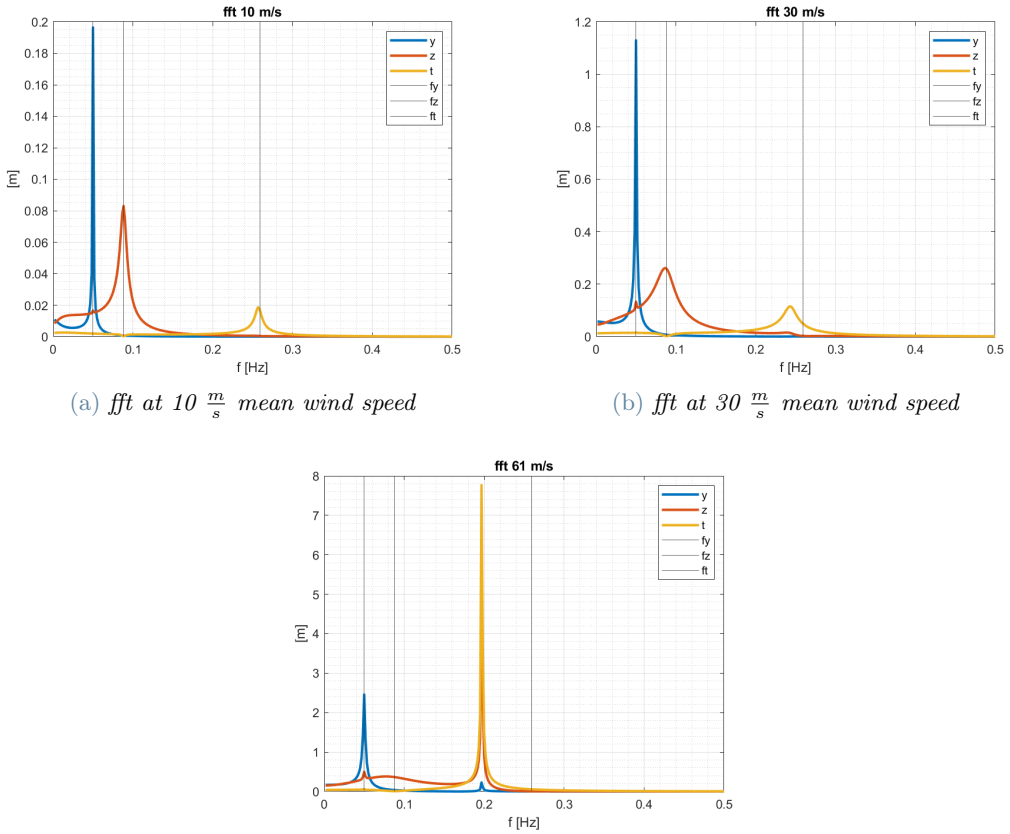

(a) *fft at 10* $\frac{m}{s}$ *mean wind speed*

(b) *fft at 30* $\frac{m}{s}$ *mean wind speed*

(c) *fft at 61* $\frac{m}{s}$ *mean wind speed*

Figure 6: FFT sectional model

A better description of the phenomenon is given by the Power Spectral Density (PSD), which represents the frequency content of the signal and the energy associated. In figure **??** PSD plots are reported. Also in this case, as done for figure 6, three different situations are reported highlighting the different behaviour of the degrees of freedom at different mean wind speeds. Indeed, far from the instability condition the frequencies are equal to the natural ones and, increasing the mean wind speed, the coupled degrees of freedom [2] have frequencies

[2] As commonly happens in structures close to dynamic instability situations the vertical motion is aerodinamically

closer one to the other the closer we are to the instability conditions. Indeed, at the flutter wind speed, those frequencies are almost equal and a high amount of energy associated to those motions is shown.

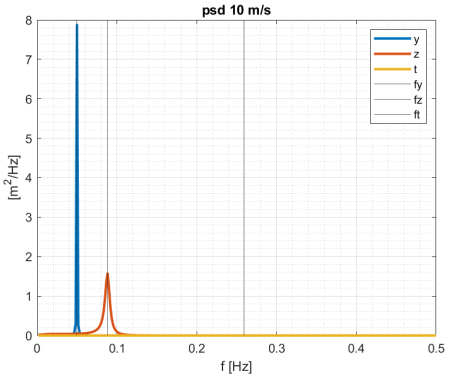

(a) *PSD at 10* $\frac{m}{s}$ *mean wind speed*

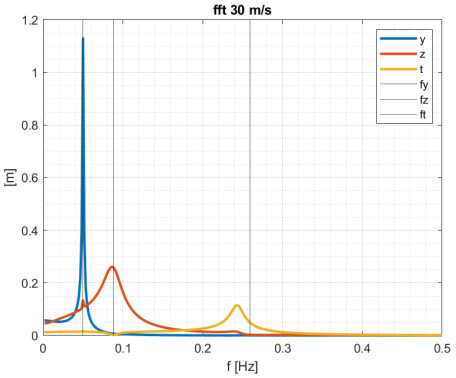

(b) *PSD at 30* $\frac{m}{s}$ *mean wind speed*

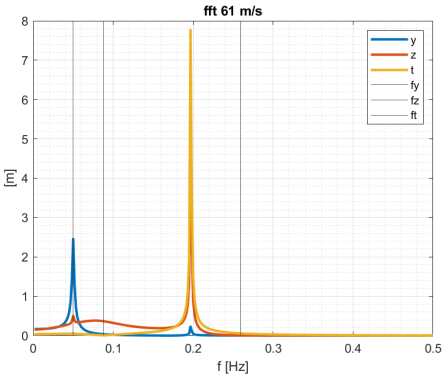

(c) *PSD at 61* $\frac{m}{s}$ *mean wind speed*

Figure 7: PSD sectional model

The energy content of a signal is expressed as the area underneath the PSD plot. Indeed, it is well known that white noise, which is by definition an infinite energy signal, is characterized by a constant PSD; hence the area covered by the plot is infinite.
Computing the surface covered by the previously cited plot we have the amount of energy at each mean wind speed analyzed. Hence, we can represent in figure 8 the energy content of each motion in function of the mean wind speed obtaining, once again, the flutter condition at $61\frac{m}{s}$, i.e. the wind speed at which instabilities occur due to the huge amount of energy injected in the system. We could have analyzed a wider wind speed range to identify the successive flutter speeds, but these are not important in aeroelastic consideration because they would never be reached in real situations.

coupled to the twist of the section (motions defined as *Plunge* and *Pitch*) due to the quasi-steady approach used in the aeroelastic analysis of the system.

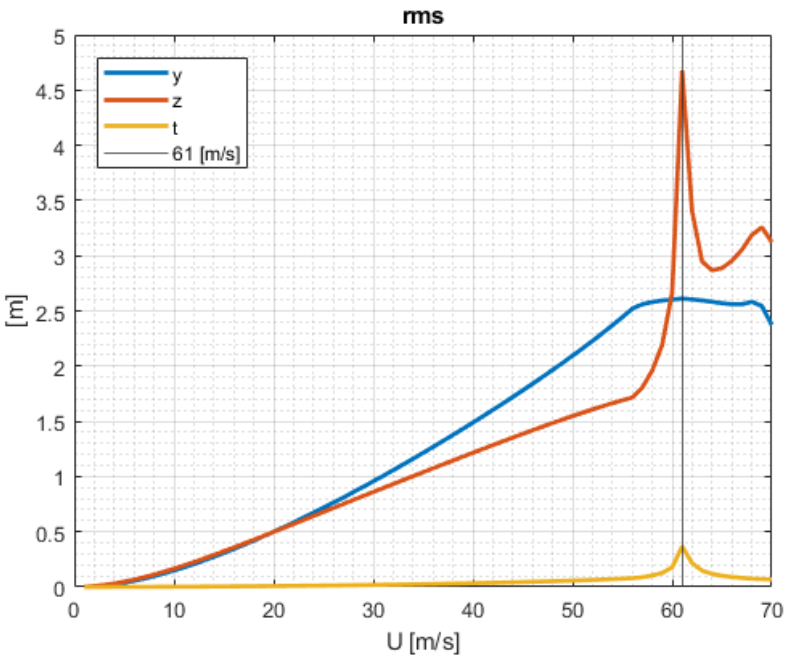

Figure 8: Root Mean Square of the PSD plot in function of the wind mean speed

3.3. Full bridge's static and dynamic response

The full bridge's dynamic was computed using a modal approach. By superimposing the modes for every section we were able to retrieve the full dynamics. In particular, we focused our attention on the first 14 modes to have an accurate characterization of the real system. In a way similar to the sectional approach static displacements have been computed and they are reported at different wind speeds in figure 9.

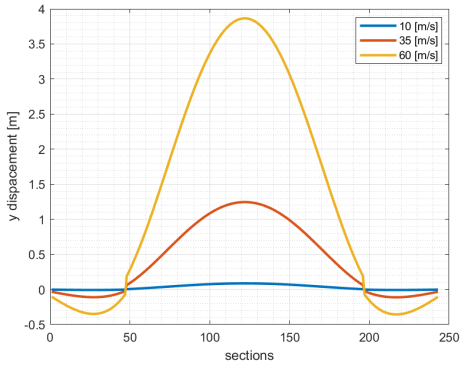

(a)

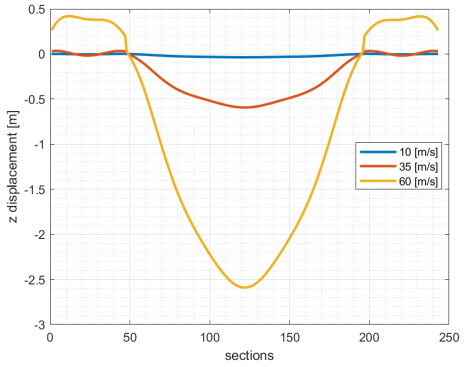

(b)

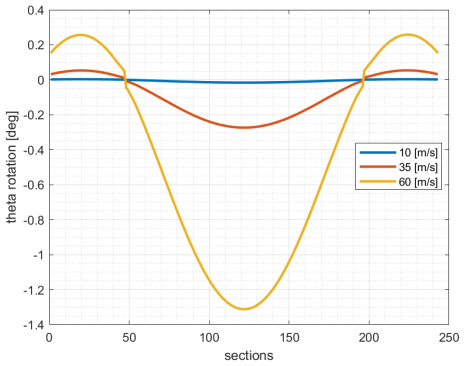

(c)

Figure 9: Static displacement

In the picture 10 we can identify the same behaviour of the eigenvalues in the sectional problem: some of them turn negative, leading to instability. On the right, we highlighted the modes whose eigenvalues' real parts turn positive, as previously said.

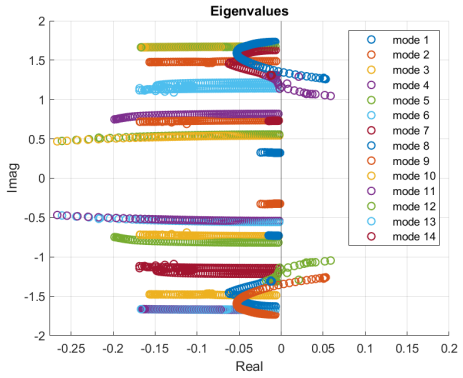

(a)

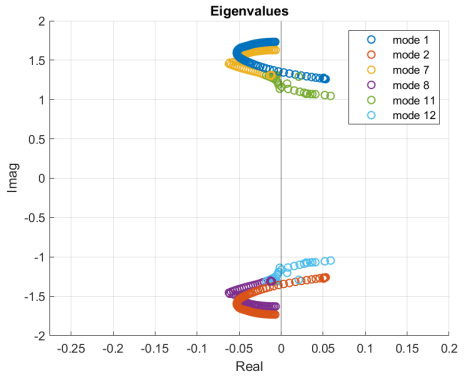

(b)

Figure 10: Full bridge's eigenvalues

When the damping ratio turns negative for at least one mode, instability occurs, so in figure 11 are plotted the damping for each mode with a focus on the vibrational modes in which damping turns negative earlier. Following the considerations reported for the sectional model, the flutter speed is identified at about 67 $\frac{m}{s}$. This value is higher than the one computed for the sectional model due to the stabilizing effect due to the mutual interaction of consecutive bridge sections, from both aerodynamic and structural points of view.

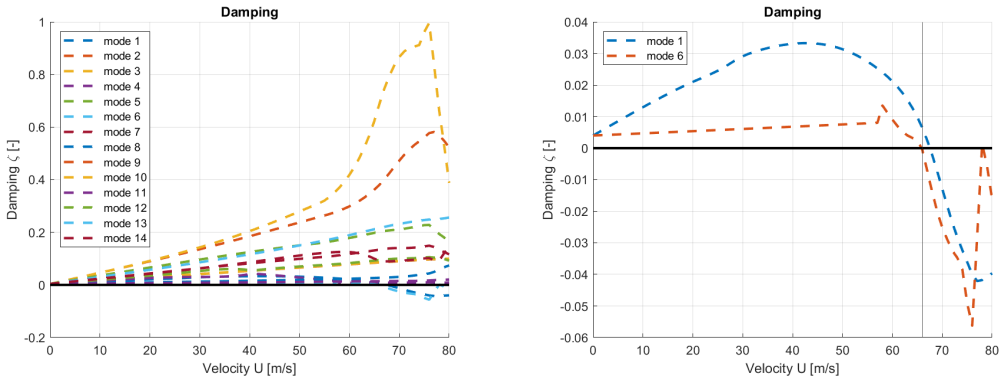

(a) (b)

Figure 11: Full bridge's damping ratios